



Supplement of

Evapotranspiration in the Amazon: spatial patterns, seasonality, and recent trends in observations, reanalysis, and climate models

Jessica C. A. Baker et al.

Correspondence to: Jessica C. A. Baker (j.c.baker@leeds.ac.uk)

The copyright of individual parts of the supplement might differ from the article licence.

Contents

Table S1 – River gauge station data.

Table S2 – Seasonal variation in catchment-balance error estimates.

Table S3 – Details of the 13 CMIP5 models analysed in this study.

Table S4 – Details of the 10 CMIP6 models included in study.

Table S5 – Data for the six LBA flux tower sites used in the study.

Table S6 – Sensitivity of K34 seasonal correlations to changing data-inclusion thresholds.

Table S7 – Table of catchment-mean ET estimates.

Figure S1 – Comparing ET estimates based on water-budget analysis.

Figure S2 – Relative uncertainty in Amazon catchment-balance ET estimates.

Figure S3 – Seasonal variation in components of the water-budget equation.

Figure S4 – Interannual variation in components of the water-budget equation.

Figure S5 – Kolmogorov-Smirnov analysis.

Figure S6 – Climatological mean annual ET from GLEAM

Figure S7 – Comparing catchment-mean ET estimates.

Figure S8 – Annual precipitation, radiation and leaf area index from satellites, reanalysis and climate models.

Figure S9 – Climatological seasonal cycle in ET at the K34 flux tower site.

Figure S10 – Seasonal variation in controls on ET.

Figure S11 – Seasonal variation in leaf area index over the Amazon.

Figure S12 – Climatological seasonal cycles in evapotranspiration over the northern and southern Amazon.

Figure S13 – Controls on interannual variation in Amazon ET.

Tables

Table S1 – River-gauge station data. Data for the eleven river-gauge stations used in the study.

| River catchment | Part of Amazon drained | Area (km ²) | Station name | Station code | Degrees E (°) | Degrees N (°) | Years of data |
|-----------------|------------------------|-------------------------|-----------------------|--------------|---------------|---------------|---------------|
| Amazon | 77% of basin | 4,694,100 | Óbidos | 17050001 | −55.51 | −1.91 | 1968–2019 |
| Aripuanã | S | 134,100 | Prainha Velha | 15830000 | −60.66 | −7.17 | 2002–2016 |
| Branco | N | 130,800 | Caracaráí | 14710000 | −61.13 | 1.81 | 1967–2018 |
| Japura | NW | 207,100 | Villa Bittencourt | 12845000 | −69.42 | −1.49 | 1980–2020 |
| Jari | NE | 48,900 | São Francisco | 19150000 | −52.56 | −0.57 | 1968–2014 |
| Madeira | S/SW | 1,006,200 | Porto Velho | 15400000 | −63.92 | −8.76 | 1967–2020 |
| Negro | N | 290,400 | Serrinha | 14420000 | −64.80 | −0.43 | 1977–2018 |
| Purus | S | 227,600 | Lábrea | 13870000 | −64.79 | −7.23 | 1931–2017 |
| Solimões | W | 1,192,200 | São Paulo de Olivença | 11400000 | −68.79 | −3.46 | 1973–2020 |
| Tapajós | SE | 462,700 | Buburé | 17710000 | −56.32 | −4.59 | 2004–2019 |
| | | | Itaituba | 17730000 | | | |
| Xingu | SE | 463,200 | Altamira | 18850000 | −52.21 | −3.20 | 1968–2014 |

Table S2 – Seasonal variation in Amazon catchment-balance error estimates. Absolute uncertainties (in mm) in precipitation (σ_P), river runoff (σ_R), change in groundwater storage ($\sigma_{\frac{dS}{dt}}$), and evapotranspiration (σ_{ET}), and the relative uncertainty (in %) in evapotranspiration (v_{ET}). σ_P was estimated as the random error (σ_{P_random}) plus the systematic error (σ_{P_bias}), combined in quadrature. σ_{P_random} was calculated following Eq. (4), from Huffman (1997): $\sigma_{P_random} = \bar{r} \left[\frac{H-p}{pN} \right]^{\frac{1}{2}}$ where \bar{r} is the climatological mean precipitation over the basin, H is a constant (1.5), p is the frequency of non-zero rainfall and N is the number of independent precipitation samples (defined as the number of Amazon pixels with finite P measurements in each month). For σ_{P_bias} , we used the value of −3.6 % from Table 4 in Paredes-Trejo et al. (2017). σ_R was estimated as 5% of monthly river flow (Dingman, 2015). Uncertainty in groundwater storage was quantified by combining GRACE measurement errors and leakage errors in quadrature. For these, we used Amazon-specific values from the literature (6.1 and 0.9 mm for measurement and leakage errors, see Table 1 in Wiese et al. (2016)). Since $\frac{dS}{dt}$ values were calculated using data from two consecutive months, groundwater error values were multiplied by $\sqrt{2}$ to obtain $\sigma_{\frac{dS}{dt}}$ (e.g. Maeda et al., 2017). σ_{ET} was estimated using $\sigma_{ET} = \sqrt{\sigma_P^2 + \sigma_R^2 + \sigma_{\frac{dS}{dt}}^2}$, and $v_{ET} = \frac{\sigma_{ET}}{ET} \times 100$. For further details please see the main paper. The Amazon region considered for this analysis is indicated by blue hatching in Figure 1.

| | σ_P , | σ_R | $\sigma_{\frac{dS}{dt}}$ | σ_{ET} | v_{ET} |
|-------------|--------------|------------|--------------------------|---------------|----------|
| Jan | 8.98 | 3.91 | 8.72 | 13.15 | 14.82 |
| Feb | 8.70 | 4.59 | 8.72 | 13.17 | 20.83 |
| Mar | 9.84 | 5.54 | 8.72 | 14.30 | 16.78 |
| Apr | 8.43 | 6.19 | 8.72 | 13.64 | 23.03 |
| May | 7.21 | 6.66 | 8.72 | 13.14 | 20.78 |
| Jun | 4.91 | 6.57 | 8.72 | 11.99 | 25.05 |
| Jul | 4.08 | 6.23 | 8.72 | 11.48 | 18.08 |
| Aug | 3.67 | 5.41 | 8.72 | 10.92 | 11.32 |
| Sep | 4.25 | 4.13 | 8.72 | 10.58 | 8.79 |
| Oct | 5.74 | 3.11 | 8.72 | 10.91 | 8.85 |
| Nov | 6.98 | 2.81 | 8.72 | 11.50 | 10.67 |
| Dec | 8.35 | 3.23 | 8.72 | 12.43 | 13.53 |
| Mean | 6.76 | 4.87 | 8.72 | 12.27 | 16.04 |

Table S3 – Details of the 13 CMIP5 models analysed in this study. Models that provided historical simulations of evapotranspiration, precipitation, surface radiation and leaf area index over the historical period were selected.

| | Modelling centre | Model | Native resolution (°) |
|----|---|--------------|-----------------------|
| 1 | Commonwealth Scientific and Industrial Research Organization (CSIRO) and Bureau of Meteorology (BOM), Australia | ACCESS1-3 | 1.875 x 1.25 |
| 2 | Beijing Climate Centre, China Meteorological Administration | bcc-csm1-1 | 2.8125 x 2.8125 |
| 3 | College of Global Change and Earth System Science, Beijing Normal University | BNU-ESM | 2.8125 x 2.8125 |
| 4 | Canadian Centre for Climate Modelling and Analysis | CanESM2 | 2.8125 x 2.8125 |
| 5 | National Centre for Atmospheric Research | CCSM4 | 1.25 x 0.9375 |
| 6 | Community Earth System Model Contributors | CESM1-BGC | 1.25 x 0.9375 |
| 7 | The First Institute of Oceanography, SOA, China | FIO-ESM | 2.8125 x 2.8125 |
| 8 | Met Office Hadley Centre | HadGEM2-CC | 1.875 x 1.25 |
| 9 | | HadGEM2-ES | 1.875 x 1.25 |
| 10 | Institute for Numerical Mathematics | inmcm4 | 2 x 1.5 |
| 11 | Institut Pierre-Simon Laplace | IPSL-CM5A-LR | 3.75 x 1.875 |
| 12 | Max-Planck-Institut für Meteorologie (Max Planck Institute for Meteorology) | MPI-ESM-LR | 1.875 x 1.875 |
| 13 | Norwegian Climate Centre | NorESM1-M | 2.5 x 1.875 |

Table S4 – Details of the 10 CMIP6 models analysed in this study. Models that provided historical simulations of evapotranspiration, precipitation, surface radiation and leaf area index were selected.

| | Modelling centre | Model | Native resolution (°) |
|----|--|-----------------|-----------------------|
| 1 | Commonwealth Scientific and Industrial Research Organization (CSIRO) | ACCESS-ESM1-5 | 1.875 x 1.25 |
| 2 | Beijing Climate Centre, China Meteorological Administration | BCC-CSM2-MR | 1.125 x 1.125 |
| 3 | | BCC-ESM1 | 2.8125 x 2.8125 |
| 4 | Community Earth System Model Contributors | CESM2 | 1.25 x 0.9375 |
| 5 | | CESM2-WACCM | 1.25 x 0.9375 |
| 6 | NASA Goddard Institute for Space Studies | GISS-E2-1-G | 2.5 x 2 |
| 7 | Met Office Hadley Centre | HadGEM3-GC31-LL | 1.875 x 1.25 |
| 8 | | HadGEM3-GC31-MM | 0.833 x 0.556 |
| 9 | Seoul National University, Seoul, South Korea | SAM0-UNICON | 1.25 x 0.9375 |
| 10 | Met Office Hadley Centre | UKESM1-0-LL | 1.875 x 1.25 |

Table S5 – Data for the six LBA flux tower sites used in the study.

| Site code | Site name | Latitude | Longitude | Land cover type | Years of data |
|-----------|--|----------|-----------|----------------------------|---------------|
| BAN | Bananal, Tocantins State | -9.82 | -50.15 | Seasonally flooded ecotone | 2003–2006 |
| K34 | km 34, Manaus | -2.61 | -60.21 | Forest | 1999–2017 |
| K67 | km 67, Santarém | -2.85 | -54.97 | Primary forest | 2002–2006 |
| K83 | km 83, Santarém | -3.05 | -54.93 | Selectively logged forest | 2000–2004 |
| RJA | Reserva Jaru Tower A, Rondônia State | -10.08 | -61.93 | Tropical dry forest | 1999–2002 |
| PDG | Reserva Pé-de-Gigante, São Paulo State | -21.62 | -47.63 | Cerrado/savanna | 2002–2003 |

Table S6 – Sensitivity of K34 seasonal correlations to changing data-inclusion thresholds. Testing the sensitivity of seasonal correlations between K34 and gridded ET datasets to changing the data-inclusion thresholds for the K34 dataset. The left-hand column indicates the minimum number of hours of flux-tower measurements required in each day, and the minimum number of days required in each month, to compute monthly-mean ET values.

| | Dataset | MODIS | P-LSH | GLEAM | ERA5 | CMIP5 | CMIP6 |
|---------------------|----------|-------------|-------------|-------|-------------|-------|-------|
| 0hrs_0days | r | 0.77 | 0.67 | 0.16 | 0.55 | -0.31 | -0.06 |
| | p | 0.00 | 0.02 | 0.62 | 0.07 | 0.32 | 0.84 |
| 0hrs_10days | r | 0.78 | 0.67 | 0.31 | 0.54 | -0.28 | -0.1 |
| | p | 0.00 | 0.02 | 0.33 | 0.07 | 0.37 | 0.75 |
| 0hrs_21days | r | 0.77 | 0.61 | 0.23 | 0.47 | -0.21 | 0 |
| | p | 0.00 | 0.04 | 0.46 | 0.12 | 0.52 | 0.99 |
| 18hrs_0days | r | 0.8 | 0.71 | 0.1 | 0.59 | -0.43 | -0.09 |
| | p | 0.00 | 0.01 | 0.75 | 0.04 | 0.16 | 0.79 |
| 18hrs_10days | r | 0.77 | 0.72 | 0.34 | 0.61 | -0.36 | -0.16 |
| | p | 0.00 | 0.01 | 0.29 | 0.04 | 0.25 | 0.62 |
| 18hrs_21days | r | 0.67 | 0.51 | 0.12 | 0.43 | -0.32 | 0.03 |
| | p | 0.02 | 0.09 | 0.7 | 0.17 | 0.31 | 0.93 |
| 21hrs_0days | r | 0.8 | 0.71 | 0.21 | 0.59 | -0.44 | -0.08 |
| | p | 0.00 | 0.01 | 0.5 | 0.04 | 0.16 | 0.81 |
| 21hrs_10days | r | 0.74 | 0.72 | 0.3 | 0.65 | -0.4 | -0.21 |
| | p | 0.01 | 0.01 | 0.35 | 0.02 | 0.19 | 0.52 |
| 21hrs_21days | r | 0.7 | 0.56 | 0.03 | 0.5 | -0.44 | -0.04 |
| | p | 0.01 | 0.06 | 0.92 | 0.1 | 0.15 | 0.91 |

Table S7 – Table of catchment-mean ET estimates. The climatological annual and interannual standard deviation (σ) in ET over each catchment for each of the ET data sources in this study (mm year^{-1}). Correlations between catchment-balance ET and other ET estimates are shown. All data are from 2003–2013, apart from the CMIP5 data, which are from 1994–2004. These data are shown in a scatter plot in Figure S7.

| | Catchment-balance | MODIS | P-LSH | GLEAM | ERA5 | CMIP5 | CMIP6 |
|--|--------------------|-------------------|-------------------|-------------------|--------------------|--------------------|--------------------|
| Catchment | Mean $\pm \sigma$ | Mean $\pm \sigma$ | Mean $\pm \sigma$ | Mean $\pm \sigma$ | Mean $\pm \sigma$ | Mean $\pm \sigma$ | Mean $\pm \sigma$ |
| Amazon | 1083.1 \pm 36.5 | 1298.7 \pm 27.2 | 1266.8 \pm 16.5 | 1480.8 \pm 16.4 | 1279.7 \pm 8.0 | 1244.0 \pm 16.8 | 1298.7 \pm 15.9 |
| Aripuanã | 1403.3 \pm 81.0 | 1409.1 \pm 32.4 | 1348.4 \pm 29.0 | 1500.4 \pm 36.8 | 1239.1 \pm 33.6 | 1236.2 \pm 33.8 | 1293.7 \pm 31.5 |
| Branco | 1087.2 \pm 117.0 | 1187.2 \pm 24.1 | 1247.5 \pm 14.7 | 1472.0 \pm 61.9 | 1213.5 \pm 39.7 | 1049.2 \pm 45.8 | 1066.3 \pm 47.9 |
| Japura | 1217.0 \pm 158.4 | 1339.4 \pm 51.4 | 1263.2 \pm 19.8 | 1632.9 \pm 24.7 | 1340.0 \pm 17.5 | 1421.9 \pm 26.8 | 1386.9 \pm 24.8 |
| Jari | 1487.0 \pm 107.3 | 1501.0 \pm 36.4 | 1439.9 \pm 16.2 | 1793.2 \pm 62.8 | 1074.4 \pm 68.9 | 1032.6 \pm 59.1 | 1002.8 \pm 72.4 |
| Madeira | 1011.4 \pm 43.2 | 1185.8 \pm 27.1 | 1131.1 \pm 14.1 | 1196.4 \pm 38.1 | 1198.6 \pm 18.4 | 1063.2 \pm 22.1 | 1154.9 \pm 24.9 |
| Negro | 1206.1 \pm 85.3 | 1338.4 \pm 51.9 | 1361.5 \pm 16.9 | 1727.7 \pm 25.1 | 1367.3 \pm 14.8 | 1429.1 \pm 31.8 | 1448.6 \pm 28.0 |
| Purus | 1248.0 \pm 109.1 | 1406.1 \pm 46.4 | 1336.1 \pm 30.9 | 1538.8 \pm 38.3 | 1305.6 \pm 18.8 | 1224.8 \pm 32.8 | 1340.8 \pm 26.2 |
| Solimões | 966.6 \pm 138.9 | 1239.6 \pm 39.7 | 1209.7 \pm 17.2 | 1436.1 \pm 15.1 | 1239.4 \pm 10.6 | 1245.1 \pm 18.6 | 1269.0 \pm 18.4 |
| Tapajós | 1180.7 \pm 96.7 | 1291.2 \pm 31.2 | 1265.6 \pm 38.2 | 1382.6 \pm 44.5 | 1238.8 \pm 28.5 | 1178.1 \pm 30.4 | 1256.9 \pm 33.2 |
| Xingu | 1445.0 \pm 130.9 | 1336.2 \pm 27.3 | 1306.9 \pm 40.9 | 1414.8 \pm 39.3 | 1238.0 \pm 21.2 | 1173.2 \pm 33.1 | 1226.7 \pm 32.3 |
| Correlation with catchment-balance ET | | r=0.84, p=0.00 | r=0.82, p=0.00 | r=0.51, p=0.11 | r=-0.28, p=0.41 | r=-0.06, p=0.85 | r=-0.14, p=0.69 |

Figures

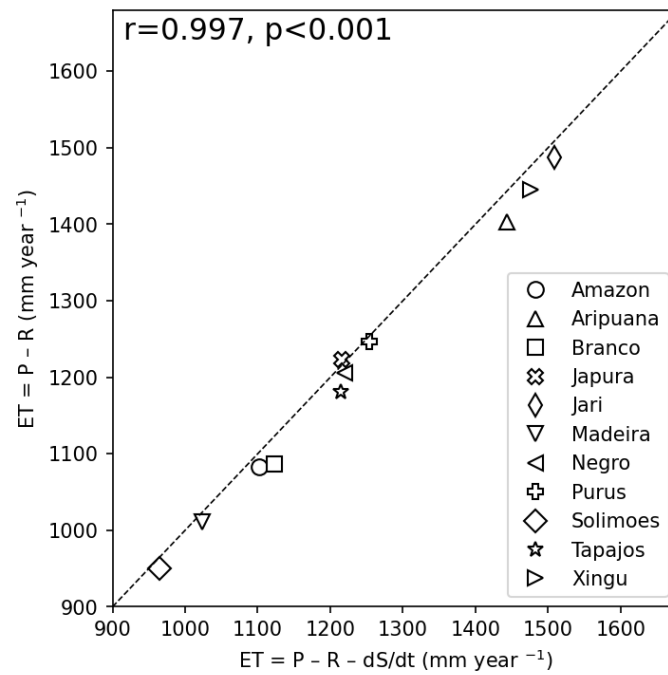


Figure S1 – Comparing ET estimates based on water-budget analysis. Relationship between climatological annual mean ET estimated from precipitation (P), runoff (R), and change in terrestrial water storage (dS/dt), and ET estimated from P and R only, over the Amazon and ten sub-catchments. Data are from 2003–2013.

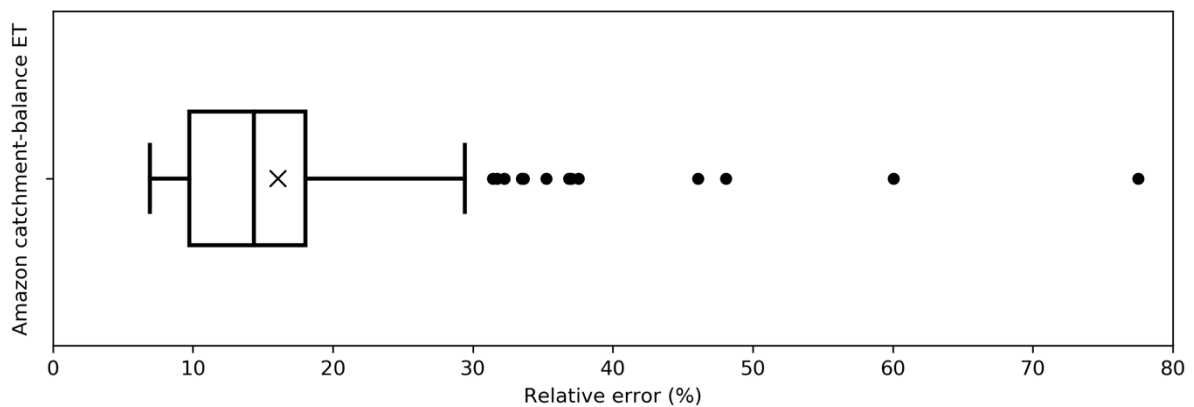


Figure S2 – Relative uncertainty in Amazon catchment-balance ET estimates. Distribution of relative errors in monthly Amazon catchment balance ET from 2003–2013.

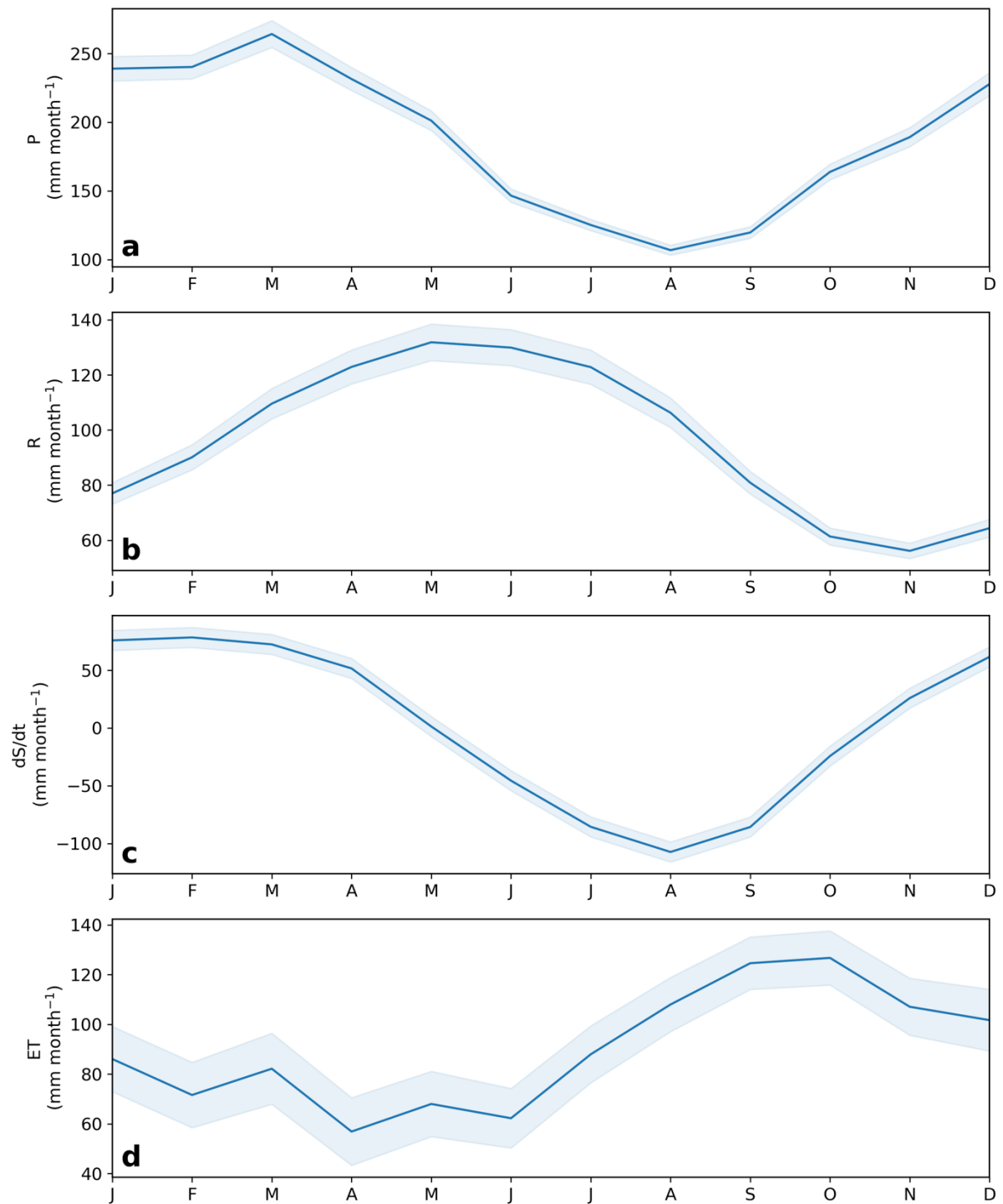


Figure S3 – Seasonal variation in components of the water-budget equation. a) Precipitation (P); b) river runoff (R); c) change in groundwater storage (dS/dt); and d) evapotranspiration (ET). Shading represents the mean absolute error in each month.

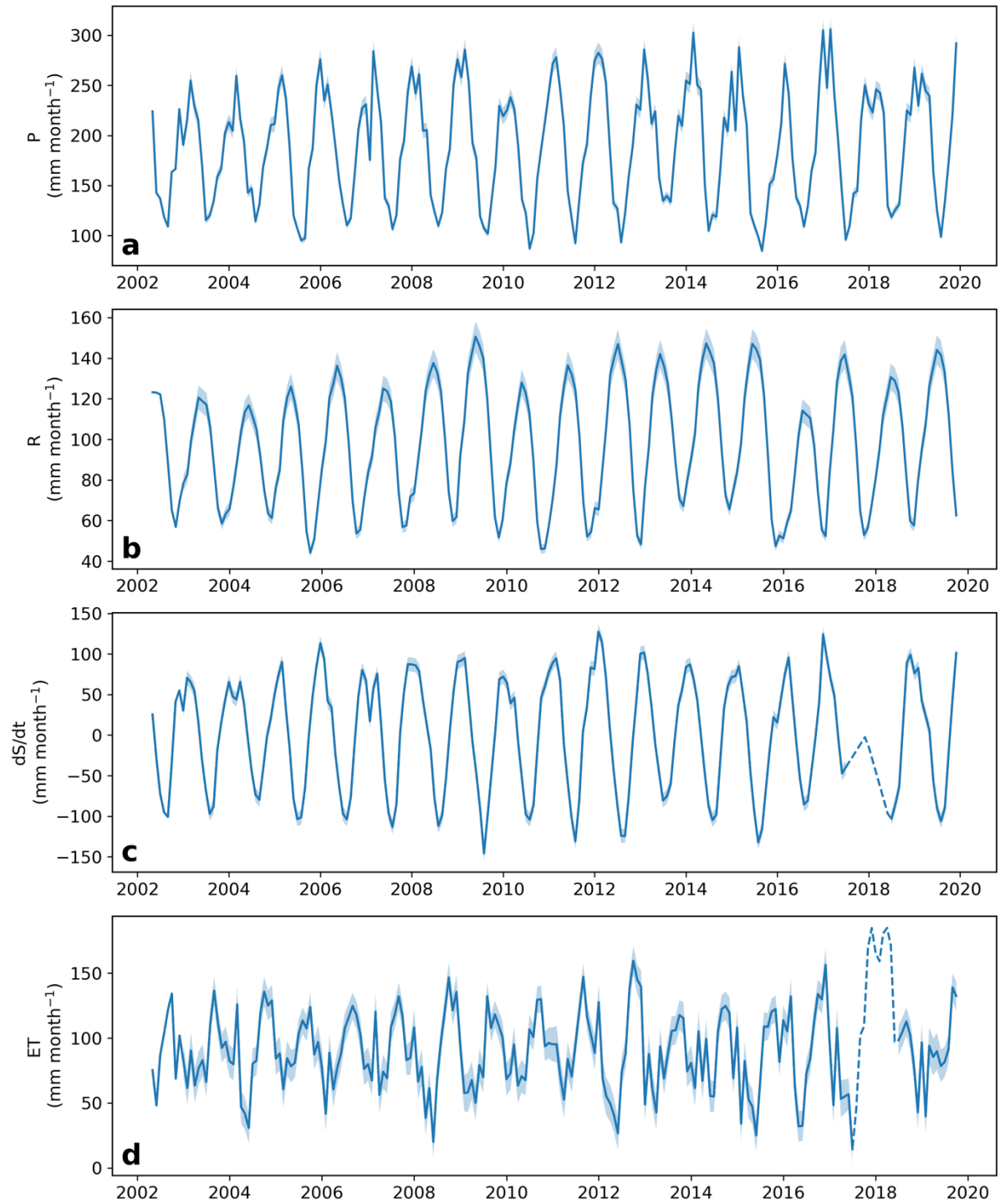


Figure S4 – Interannual variation in components of the water-budget equation. a) Precipitation (P); b) river runoff (R); c) change in groundwater storage (dS/dt); and d) evapotranspiration (ET). Shading represents the absolute error in each month. Dashed lines indicate data that were removed due to doubts over reliability.

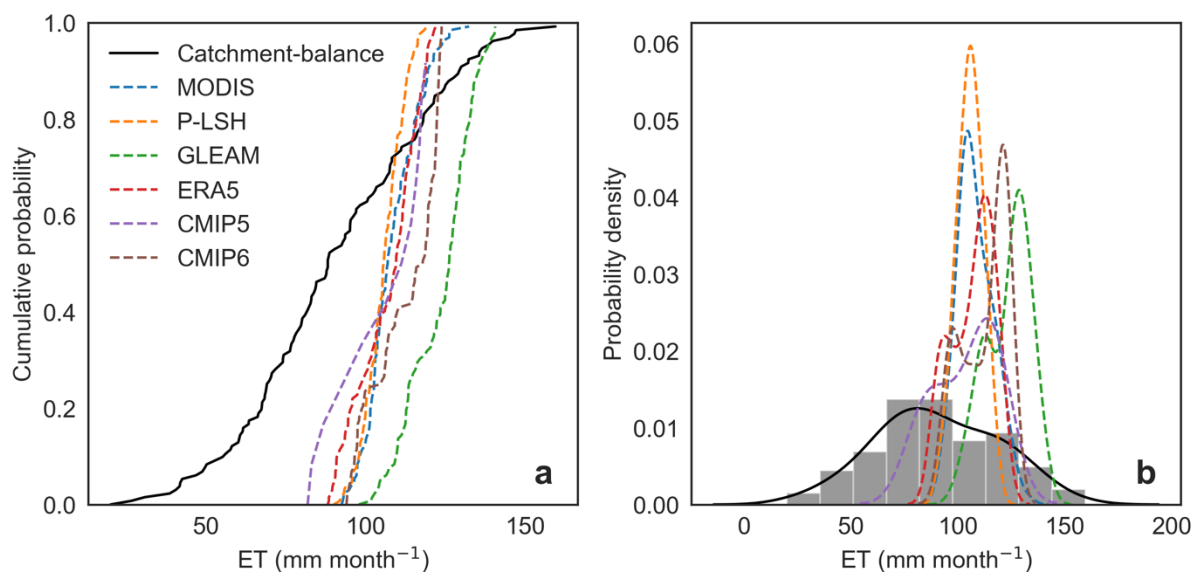


Figure S5– Kolmogorov-Smirnov analysis. The cumulative probability (a) and probability density (b) functions for monthly Amazon ET from catchment-balance, satellites (MODIS, P-LSH, GLEAM), ERA5 reanalysis, and climate models (CMIP5 and CMIP6) from 2003 to 2013. Dashed lines indicate the data come from a statistically different distribution from the catchment-balance data (determined using a two-sample Kolmogorov-Smirnov test).

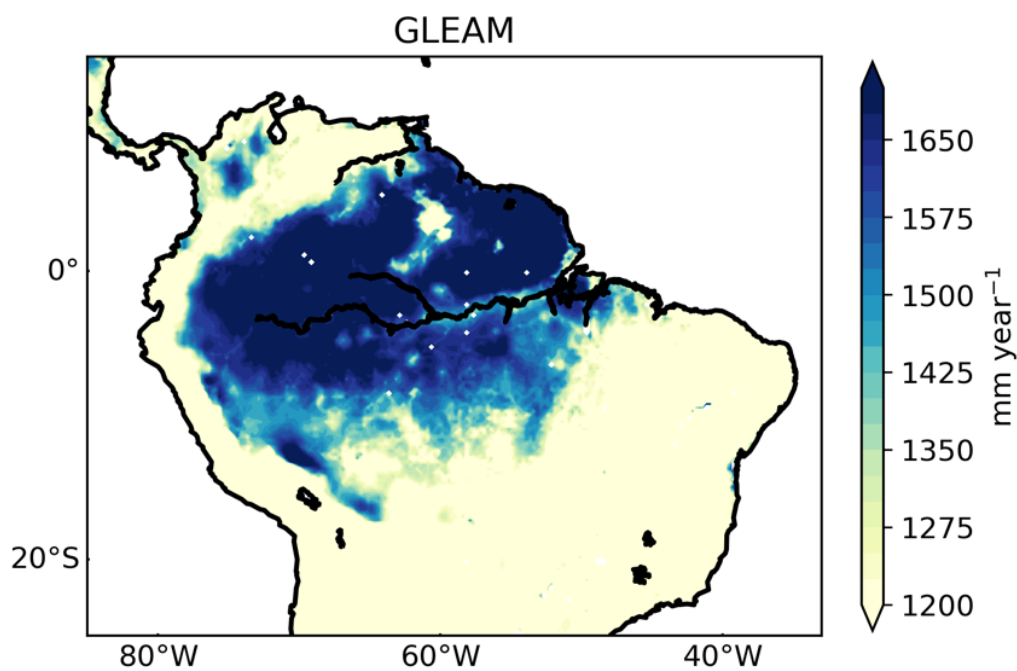


Figure S6 – Climatological mean annual ET from GLEAM (2003–2013).

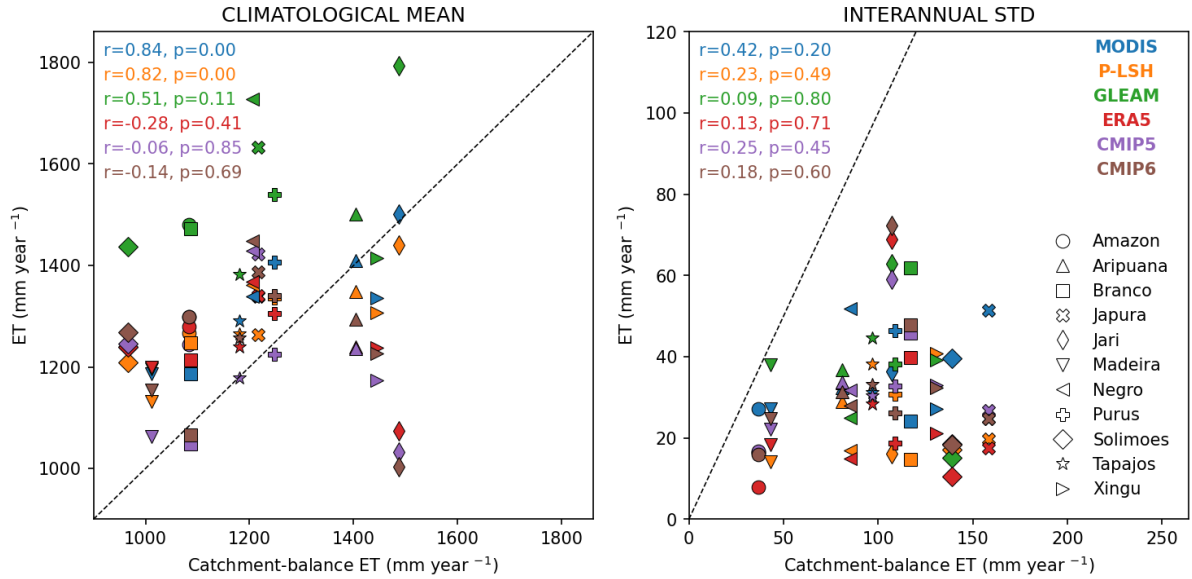


Figure S7 – Comparing catchment-mean ET estimates. The climatological annual means (left panel) and standard deviations (right panel) of catchment-balance ET estimates plotted against ET estimates from six gridded products. All data are from 2003–2013, apart from the CMIP5 data, which are from 1994–2004. Catchment locations are shown in Figure 1.

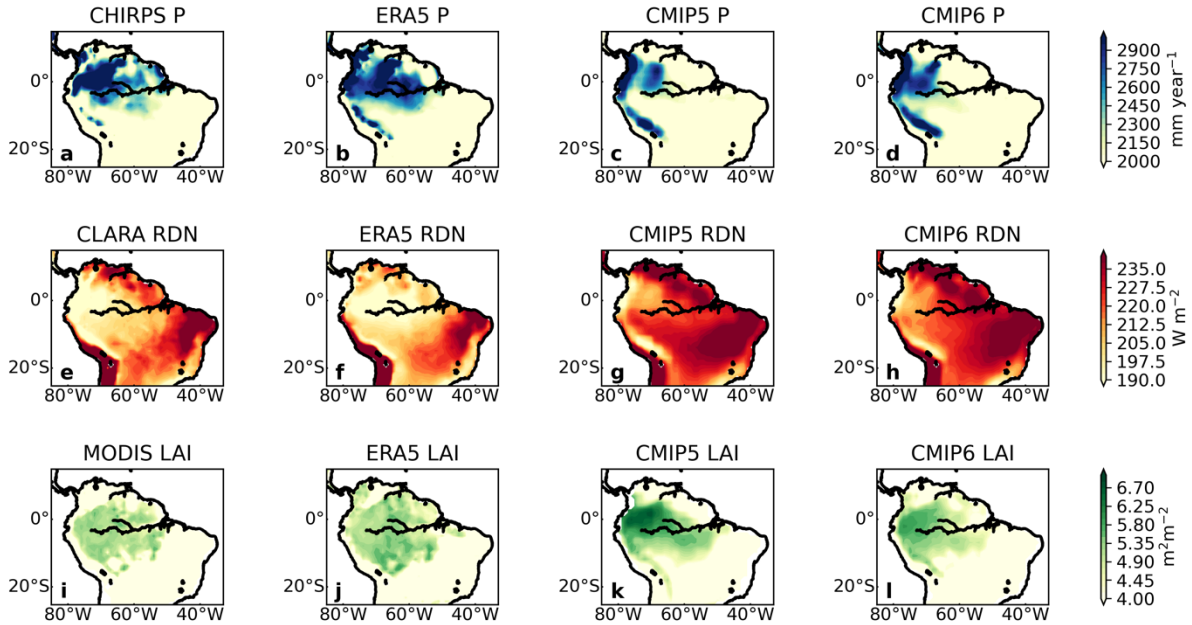


Figure S8 – Climatological annual precipitation, radiation and leaf area index. Mean annual precipitation (P, a–d), radiation (RDN, e–h) and leaf area index (LAI, i–l) from satellites (column 1), reanalysis (column 2) and climate models (columns 3 & 4) over the period 2003–2013. References for each dataset are provided in the main paper.

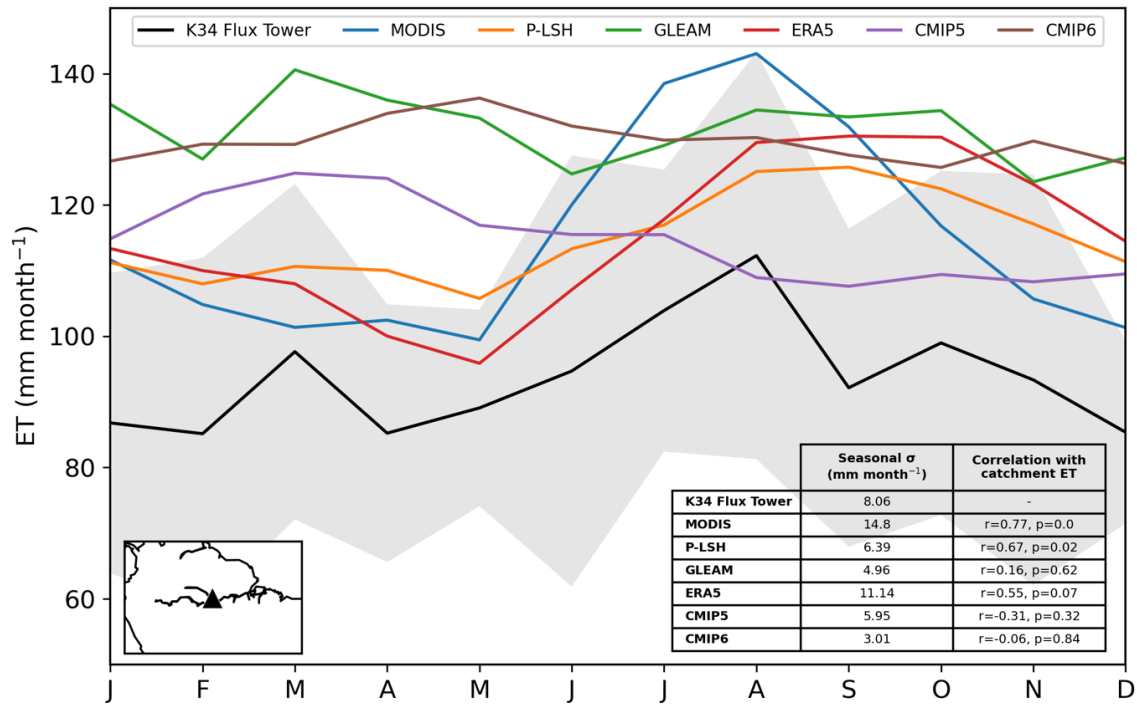


Figure S9 – Climatological seasonal cycle in ET at the K34 flux tower site. Lines indicate the seasonal time series in ET from the K34 flux tower (black), satellites (dark blue), ERA5 reanalysis (light blue) and climate models (green). The location of the K34 tower is indicated in the inset map. Data for satellite and reanalysis products were taken from a 0.25° grid cell containing the tower, and model data were from a 1° grid cell. Shading represents the standard deviation in flux-tower ET (see Methods). The inset table records the seasonal variation (standard deviation, σ) in ET for each dataset, and the correlations between each dataset and flux-tower ET. ET data from the K34 tower are from 1999–2017, data for all other products are from 2003–2013. Note that the y-axis does not start at zero.

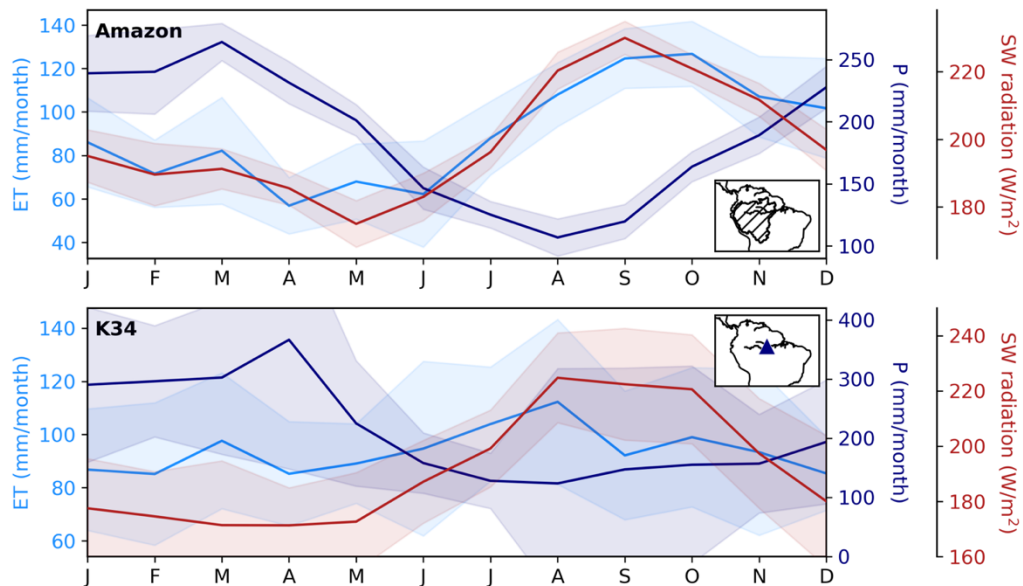


Figure S10 – Seasonal variation in controls on ET. Climatological seasonal cycles in ET (light blue), precipitation (P, dark blue) and shortwave radiation (red) averaged over the Amazon (catchment-balance data from 2003–2013, top panel) and measured at the K34 flux tower site (bottom panel, data from 1999–2017). P and radiation data for the Amazon basin are area-weighted basin-means of CHIRPS and CLARA-A1 data, respectively. Confidence intervals indicate the interannual standard deviation in each month. Note that y-axes do not all start at zero.

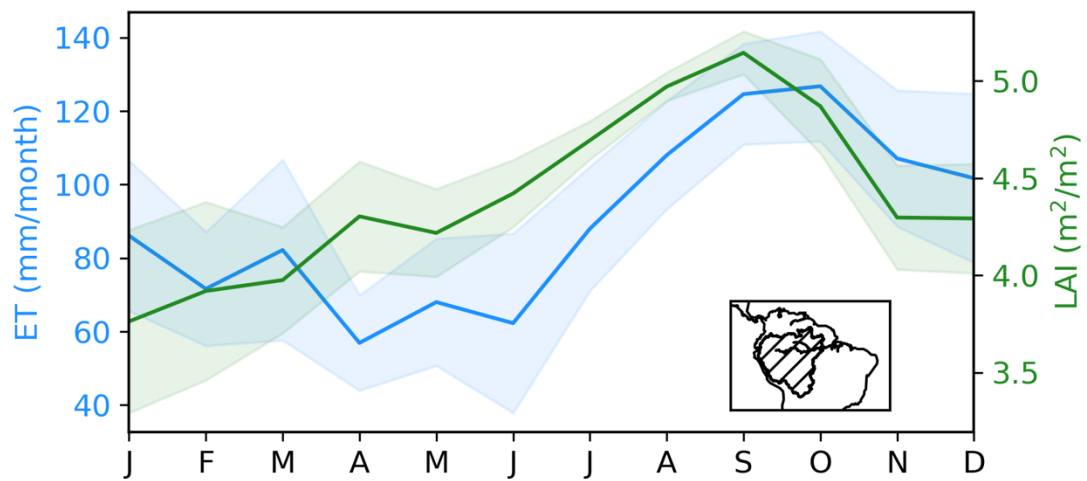


Figure S11 – Seasonal variation in leaf area index over the Amazon. Climatological seasonal cycles in catchment-balance ET (light blue) and MODIS MOD15A2H Collection 6 LAI (green) averaged over the Amazon region shown in the inset map (area-weighted mean using data from 2003–2013). Confidence intervals indicate the interannual standard deviation in each month. Note that y-axes do not start at zero.

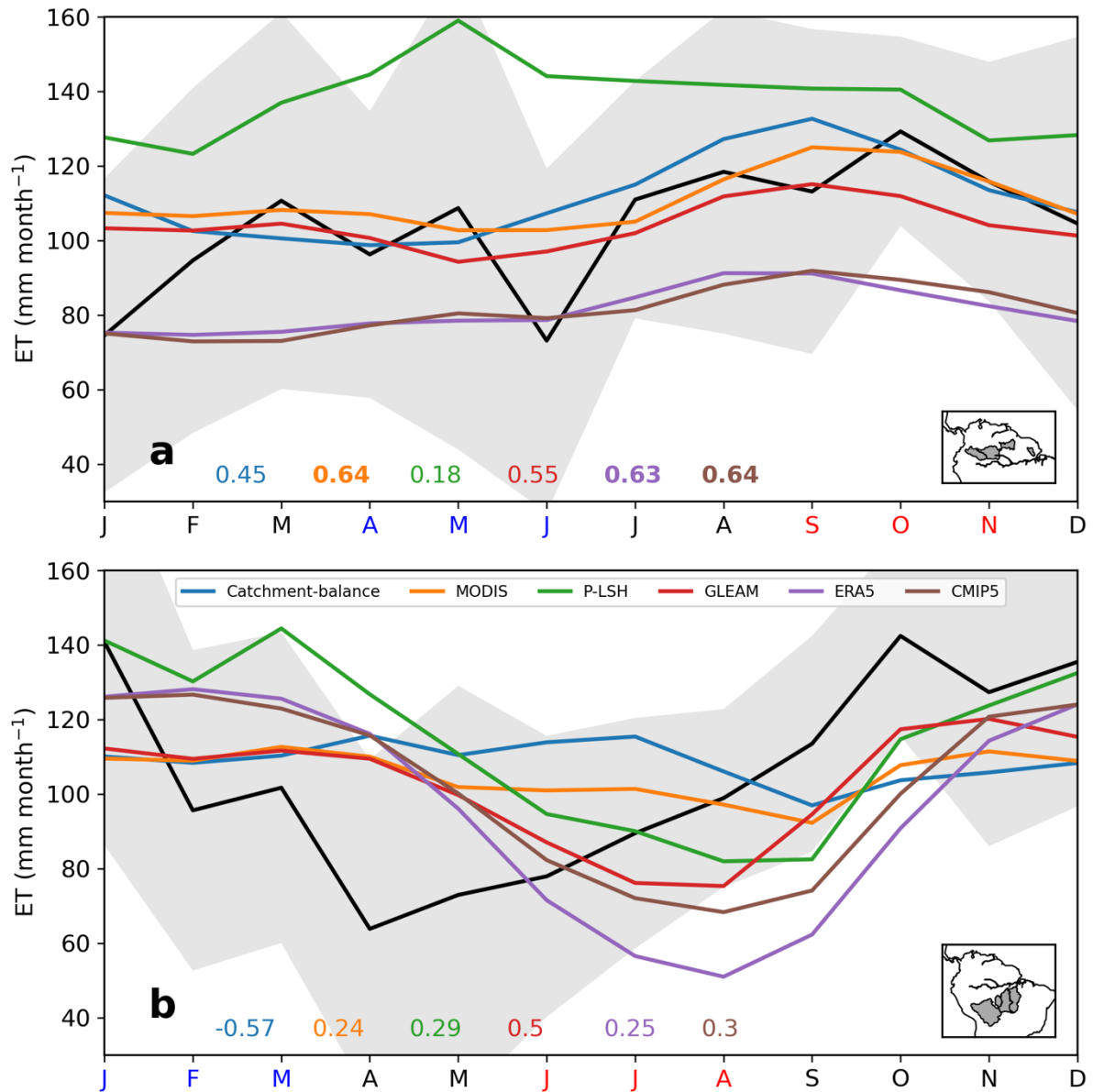


Figure S12 – Climatological seasonal cycles in evapotranspiration over the northern and southern Amazon. Mean seasonal cycle in ET from catchment balance, satellites (MODIS, P-LSH, GLEAM), ERA5 reanalysis and climate models (CMIP5 and CMIP6) over the northern Amazon basins (a) and southern Amazon basins (b). The regions used in each analysis are indicated in the inset maps. Shading represents absolute uncertainty in catchment-balance ET (see Methods). Correlations with catchment-balance ET are shown on each panel, with bold numbers indicating statistical significance ($p < 0.05$). Data are from 2003 to 2013, with the exception of CMIP5, where the data are from 1994–2004. On the x-axis of each panel, the three wettest months are indicated in blue and three driest months are indicated in red. Note that the axes do not start at zero.

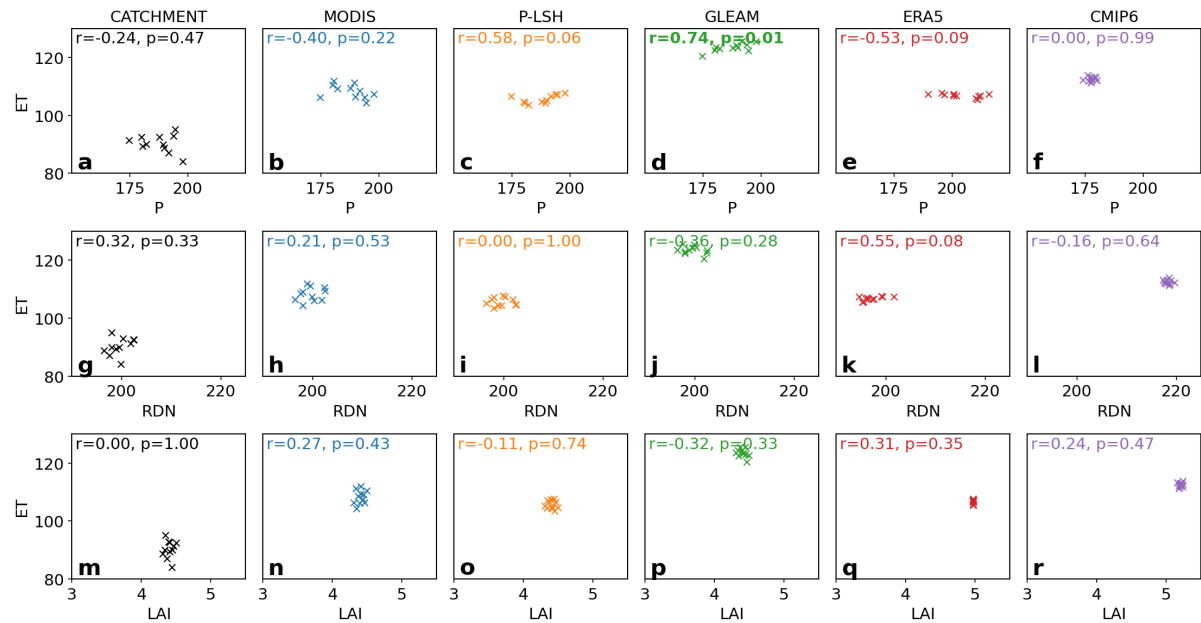


Figure S13 – Controls on interannual variation in Amazon ET. Interannual ET (in units of mm month^{-1}) for the Amazon (Fig. 1) from catchment-balance, satellites (MODIS, P-LSH, GLEAM), ERA5 reanalysis and CMIP6 plotted against (a–f) precipitation (P, mm month^{-1}); (g–l) surface shortwave radiation (RDN, W m^{-2}); and (m–r) leaf area index (LAI, $\text{m}^2 \text{m}^{-2}$). Satellite ET data are plotted against P from CHIRPS, RDN from CLARA-A1 and LAI from MODIS; ERA5 and CMIP6 ET are plotted against ERA5 and CMIP6 P, RDN and LAI, respectively. All data are from 2003 to 2013. Note that the axes do not start at zero.

Supplementary references

- Dingman, S. L. 2015. *Physical hydrology*, Waveland press.
- Huffman, G. J. 1997. Estimates of root-mean-square random error for finite samples of estimated precipitation. *Journal of Applied Meteorology*, 36, 1191-1201.
- Maeda, E. E., Ma, X. L., Wagner, F. H., Kim, H., Oki, T., Eamus, D. & Huete, A. 2017. Evapotranspiration seasonality across the Amazon Basin. *Earth System Dynamics*, 8, 439-454.
- Paredes-Trejo, F. J., Barbosa, H. A. & Lakshmi Kumar, T. V. 2017. Validating CHIRPS-based satellite precipitation estimates in Northeast Brazil. *Journal of Arid Environments*, 139, 26-40.
- Wiese, D. N., Landerer, F. W. & Watkins, M. M. 2016. Quantifying and reducing leakage errors in the JPL RL05M GRACE mascon solution. *Water Resources Research*, 52, 7490-7502.